Experimental Determination of the Dependence of OH Radical Yield on Photon Energy: A Comparison with Theoretical Simulations

J. Fulford, P. Bonner, D. T. Goodhead, M. A. Hill, and P. O'Neill*

MRC, Radiation and Genome Stability Unit, Harwell, Didcot, Oxon OX11 0RD, U.K.

Received: August 31, 1999; In Final Form: October 29, 1999

On the basis of simulations of water radiolysis, it has been postulated that the yield of OH radicals, which become homogeneously distributed, is dependent upon energy when irradiated with low-energy photons. The aim of this study is to determine experimentally the dependence of the yield of OH radicals, which escape intratrack recombination, on photon energy of incident radiation using plasmid DNA as a probe. The yields of single strand breaks (ssb) induced in plasmid DNA (pUC18) when irradiated with photons varying in energy from 0.28 keV to 1.25 MeV was determined and, when normalized relative to the yield for ^{60}Co irradiation, may be used as a measure of the yield of OH radicals escaping radiation tracks. As the photon energy decreases from 1.25 MeV to 1.5 keV the OH radical yield decreases from 0.290 to 0.072 μmol J^{-1}, respectively, in line with an increased ionization density of the radiation and hence an increasing probability of radical recombination. However, with a further decrease in photon energy from 1.5 to 0.28 keV there is an upturn in OH radical yields. Carbon-K X-rays are found to have a significantly higher yield of 0.257 μmol J^{-1} than that associated with the higher energies. The experimental dependence is compared with a number of theoretical calculations, which predict an upturn in OH radical yields between 0.1 and 1 keV. Such a dependence of OH radical yields on energy provides experimental data suitable for direct comparison with simulations, aiding their refinement and development.

Introduction

Many studies have been undertaken to model the radiation chemistry of water following the time dependent yield of primary radicals.[1−9] The majority of these models have focused on γ-rays, hard X-rays, and high-energy electrons. For those that have investigated the dependence of the radical yield on the photon energy of the radiation, it was postulated that the yield of hydroxyl radicals, generated from radiation tracks in water and which escaping intratrack recombination events to become homogeneously distributed, is dependent upon the energy of the radiation.[7−11] From simulations, the majority of intratrack radical−radical interactions, in water, occur at times $<10^{-8}$ s, after which the remaining radicals may be regarded as homogeneously distributed.[1,3] The experimentally determined yields of e^-_{aq} and hydroxyl radicals obtained by pulse radiolysis confirm that the majority of intratrack events involving water radicals are complete within 10^{-7} s.[12,13] Several simulations have postulated that the yield of homogeneously distributed hydroxyl radicals decreases as the energy of the incident photon is reduced, but with very low-energy photons, <1 keV, the yield increases.[7−9] The number of water radicals that escape recombination events within the track is therefore a reflection of the ionizing density of the radiation. To date, few studies have investigated experimentally the dependence of the yield of water radicals on photon energy, and those which have, have examined the yield of ferric ions (Fricke dosimetry), which decreases with decreasing photon energy in the range 1 MeV to 2 keV.[10,14]

Low linear energy transfer (LET) radiation, i.e., γ-rays, X-rays and high-energy electrons produce low-energy, secondary electrons that contribute approximately 30% of the absorbed dose.[15] These low-energy electrons may be simulated by characteristic ultrasoft X-rays (USX), which interact almost exclusively via the photoelectric effect, producing isolated tracks of electrons with small well-defined energies (in water >99% of these interactions are with oxygen). Carbon K X-rays generally produce a single photoelectron, while for other X-ray energies an Auger electron usually accompanies the photoelectron, as indicated in Table 1. Studies employing USX have highlighted these low-energy secondary electrons to be the predominant contributor to biologically complex DNA damage.[16−21] An increase in ionization density is generally considered to give rise to an increased proportion and complexity of damage, which is less susceptible to cellular repair processes than damage produced by more sparsely distributed ionizations.[18,22,23]

The aim of this study is to determine experimentally the dependence of the yield of hydroxyl radicals that escape intratrack recombination events in water on the photon energy of the radiation. From a modeling standpoint, this information provides experimental benchmarks against which track simulations may be compared and hence leads to subsequent refinement of these models. From a biological point of view, the ionization density associated with a specific radiation energy can be assessed as a factor determining simple versus complex molecular damage. The objectives are achieved by effectively using plasmid DNA within an aqueous solution containing a given concentration of a hydroxyl scavenger, Tris, as a probe to sample the number of hydroxyl radicals present at 10^{-6} s. Plasmid DNA reacts competitively with Tris for hydroxyl radicals to give rise[24] to readily detectable single strand breaks (ssb) whose yield is subsequently determined. The concentration of the hydroxyl scavenger used sets the lifetime of the hydroxyl radicals to 10^{-6} s, sufficiently high to ensure that the majority of homogeneously distributed radicals interact with either the scavenger or DNA in a fixed proportion and are not removed as a consequence of radical−radical interactions involving

* Corresponding author. E-mail: p.oneill@har.mrc.ac.uk. Telephone: +44 (01235) 834393. Fax: +44 (01235) 834776.

10.1021/jp993087n CCC: $18.00
Published on Web 12/07/1999

TABLE 1: Properties of Characteristic USX Interactions in Water

X-ray	photon energy (keV)	dominant electron energy (keV)		combined electron range[b] (nm)	mass attenuation coefficient[c] (cm^2/g)	attenuation length (μm)
		photo	Auger			
C_K	0.28	0.25		<7	5416	1.8
Cu_L	0.96[a]	0.42	0.52	~40	4640	2.2
Al_K	1.49	0.96	0.52	~70	1421	7.0
Ti_K	4.55[a]	4.02	0.52	~500	56.97	180

[a] Weighted average.[37] [b] Combined csda (continuous slowing down approximation) range of the two electrons (single electron for C_K X-rays).[38] Energy is generally deposited over a smaller distance due to electrons being emitted in a random direction and the tortuous path followed. [c] Values calculated using elemental coefficients.[39]

homogeneously distributed radicals including the OH radical.[1,3,25] Therefore, only those hydroxyl radicals formed within a radiation track and which subsequently escape intratrack radical−radical recombinations induce DNA ssb. Consequently, the yield of strand breaks within the DNA probe is proportional to the yield of hydroxyl radical species escaping radical−radical intratrack recombination events, a reflection of the ionization density of the track.

Experimental Section

Plasmid DNA. pUC18 (2686 base pairs) was propagated in E. coli HB101 and the DNA extracted using alkali lysis followed by purification using cesium chloride−ethidium bromide gradients.[26] The plasmid, which is >95% in the supercoiled form, is subsequently stored at 277 K in a buffer (10 mmol dm^{-3} Tris, 1 mmol dm^{-3} EDTA) at a concentration of 0.5 mg/mL. The desired Tris scavenging concentration of 0.66 mmol dm^{-3} was obtained by adding 3.3 μL of the above DNA stock to 46.7 μL of triple distilled water, resulting in a final DNA concentration of 33 ng/μL, equivalent to a base pair concentration of 51 μmol dm^{-3}.

DNA Irradiation. For each X-ray irradiation, 5 μL samples of plasmid solution were irradiated within glass-walled irradiation dishes (3 cm internal diameter) made with bases of 0.35 mg cm^{-2} (~2.5 μm thickness) of Hostaphan (poly(ethylene terephthalate), manufactured by Hoechst). A CR-39 plastic disk (2.84 cm diameter) was placed on top of the plasmid sample and was rotated to facilitate even spreading of the plasmid over the entire area. Confocal microscopic analysis[27] revealed an average thickness of the plasmid solution of 7.8 μm from six individual measurements, consistent with the calculated thickness. Two 5 μL droplets of water were placed on top of the CR-39 disk, and a steel lid was positioned on the glass dish to minimize evaporation from the sample during the course of the experiment. Prior to irradiation, the samples were cooled for 7 min using a chiller thermocirculator (Churchill Inst. Co. Ltd., Perivale, U.K.) which pumped a water/antifreeze mix through a jacket surrounding the dish, ensuring that the samples were maintained at ≤277 K for the entire course of the irradiation.[28] At this temperature the conversion of heat labile sites into single strand breaks (ssb) is minimized.[29−31] Following irradiation, the sample was recovered by removing the CR-39 disk and adding 25 μL of 10 mmol dm^{-3} Tris. The CR-39 disk was replaced and again rotated to facilitate mixing of the original plasmid solution with the additional Tris solution. The solution was subsequently recovered from both the Hostaphan and CR-39 disk surfaces using a pipet and stored on ice. Prior to electrophoresis, 15 μL of loading buffer (0.1% bromophenol blue, 30% sucrose in TBE) was added to the solution. DNA samples were subjected to electrophoresis in a 1% agarose gel in TBE at pH 7.1. These gels were run typically at 74 mV cm^{-1}, 6 mA for 17 h at 277 K.

TABLE 2: Parameters Determined for a 7.8 μm Plasmid Sample Irradiated with USX in Water

X-ray	cathode potential (kV)	discharge current (mA)	area-weighted mean intensity over sample	mean to surface dose-rate ratios	typical mean absorbed dose rates (Gy min^{-1})
C_K	1.5	3.0	0.85	0.233	~0.5
Cu_L	2.0	8.0	0.91	0.269	~0.25
Al_K	4.0	4.0	0.93	0.604	~30
Ti_K	7.0	3.0	0.91	0.978	~4

For ^{60}Co γ-irradiation 20 μL of a 33 ng/μL DNA solution was placed within a 5 mm diameter glass tube. During irradiation the tube is surrounded by ice and hence has a temperature of ≤277 K. Again, following irradiation, the sample was kept on ice and analyzed by gel electrophoresis, as described above. Experiments were also undertaken with γ irradiation utilizing the Hostaphan dishes, and these confirmed that there are no experimental discrepancies resulting from the different radiation containers used.

Following electrophoresis, the gels were stained with 30 μL of ethidium bromide (10 mg/mL) in TBE (89 mmol dm^{-3} Tris, 89 mmol dm^{-3} boric acid, 2 mmol dm^{-3} EDTA) for approximately 1 h at 277 K. The gel was then washed in water and an image obtained by visualizing the gel using a UV transilluminator and a charge-coupled device (CCD) camera. The production of a DNA single strand break in supercoiled plasmid DNA results in relaxation of the plasmid to the open circular form, which has an electrophoretic mobility different from that of the supercoiled form. Images were analyzed for the relative proportions of the different plasmid forms using Collage (Fotodyne) software. A correction factor of 1.4 is used in the quantification of the gel, as previously described to allow for the reduced binding of ethidium bromide to the supercoiled form of the plasmid.[32]

Radiation Sources. *Ultrasoft X-rays.* An MRC cold cathode discharge tube[19,33] with the appropriate transmission target was used to produce characteristic ultrasoft X-rays (C_K, Cu_L, Al_K, and Ti_K) with low Bremsstrahlung contamination (<1%). The properties of these X-rays are tabulated in Table 1. Detailed descriptions of the irradiation facility and dosimetry with the various targets are given elsewhere.[19,28,34,35] The cathode potentials and discharge currents used for these experiments are given in Table 2. The X-rays, produced by electron bombardment of the target, travel 5.4 cm through a flight tube continuously flushed with helium (hydrogen for C_K X-rays) at atmospheric pressure, irradiating the plasmid through the Hostaphan base of the dish on which the plasmid was spread. Dosimetry was carried out using air-filled ionization chambers[36] (internal diameter 0.8 cm, volume 0.1 cm^3) with a 0.248 mg cm^{-2} aluminum window for the Cu_L, Al_K, and Ti_K X-rays and a 25 μg cm^{-3} carbon window for carbon X-rays. Measurements of the ionization current were made before and after each experiment using a Keithley 616 electrometer with the ion chamber window positioned 1 mm behind an empty Hostaphan-based irradiation dish. Corrections were made for the variation in X-ray intensity across the sample. These experimentally determined correction factors for calculating the area-weighted mean intensity over the whole sample compared to that measured at the center are tabulated in Table 2. The absorbed dose rate, $\dot{D}_s$, at the incident surface of the sample can be calculated from the photon fluence rate, ϕ, using

$$\dot{D}_s = \phi\left(\frac{\mu_{en}}{\rho}\right)_{water} E$$

where $(\mu_{en}/\rho)_{water}$ is the mass energy absorption coefficient of water (the value of which is essentially identical to the mass attenuation coefficient $(\mu/\rho)_{water}$, given in Table 1) for USX photons of energy E. These ultrasoft X-rays are significantly attenuated by the sample and therefore the mean absorbed dose rate, $\dot{D}_m$, in a sample of thickness x and density ρ was calculated using

$$\dot{D}_m = \dot{D}_s \frac{1 - \exp(-(\mu/\rho)_{water}\rho x)}{(\mu/\rho)_{water}\rho x}$$

The calculated mean to surface dose rate ratios and typical mean absorbed dose rates for a 7.8 μm sample with a density of 1 g cm^{-1} are tabulated in Table 2 for the various ultrasoft X-ray energies.

High-Energy Photons. Hard X-ray studies were undertaken using two different X-ray sets. A Siemens Stabilipan 1 X-ray machine was run at 250 kV (constant potential) with a compound filter of copper and aluminum producing an X-ray spectrum with a first half-value layer of 1.2 mm of copper, giving a dose rate of 2.0 Gy min^{-1} (absorbed dose to water). Back-calculation from the half-value layer gives the mass absorption coefficient from which an average photon energy of 90 keV is calculated. A Todd Research diagnostic X-ray machine with a Machlett 50 kV X-ray tube was run at 50 kV (constant potential) with an aluminum filter producing an X-ray spectrum with a first half-value layer of 1.0 mm of Al. This was run in 30 s bursts to prevent overheating, delivering 1.5 Gy (absorbed dose to water) every 30 s. The half-value layer yields a mean photon energy of 23 keV. γ irradiation was undertaken with a ^{60}Co sealed source. Dose rates for both hard X-ray and γ irradiation were assessed using a Farmer type 2570 dosimeter with a type 2581 0.6 cm^3 ionization chamber.

The Compton process becomes increasingly important for the interaction of photons with water for energies above ~25 keV, with the energy essentially shared between the emitted electron and a second lower energy photon.

Strand Break Yield Determinations. For each radiation source, a dose response was determined for the loss of supercoiled plasmid at the specified Tris scavenging concentration for OH radicals of 0.66 mmol dm^{-3}. From the slope of this response, a D_{37} value was calculated which, assuming Poisson statistics for strand break induction, represents the radiation dose required to give on average one ssb per plasmid molecule. Assuming the average mass of a base pair is 650 Da, the yield of ssb/Gy/Da is given by

$$\frac{1}{(D_{37} \times 2686 \times 650)}$$

where 2686 is the number of base pairs for pUC18.

An indication of the comparative number of OH radicals escaping the track may be made by comparing the ratio of ssb yields for different radiations to that determined for ^{60}Co γ radiation. It is assumed that the proportion of OH homogeneously distributed radicals that interact with DNA in competition with the fixed concentration of Tris is independent of the photon energy. Therefore, the yield of ssb/Gy/Da is proportional to the OH radical yield obtained under conditions of homogeneous radical distribution, i.e., at $t > 10^{-6}$ s.

Results

In Figure 1, the dependence of loss of supercoiled plasmid on radiation dose is shown for irradiation of pUC18 plasmid DNA in the presence of 0.66 mmol dm^{-3} Tris with ^{60}Co γ radiation, 50 kV (constant potential) diagnostic X-rays, and Al_K USX at a scavenging capacity of 10^6 s^{-1}, sufficiently large for OH radicals to become homogeneously distributed. The characteristic time constant (or scavenging capacity) for the interaction of OH radicals with Tris is the product of the concentration of Tris and its rate constant for interaction with OH radicals. The latter value,[40] taken to be 1.5×10^9 dm^3 mol^{-1} s^{-1}, gives a time constant of 9.5×10^5 s^{-1}, equivalent to a mean lifetime of the OH radicals of 10^{-6} s. For this constant scavenging capacity, the yields of ssb, calculated from the slope of the dose responses, are dependent upon the energy of the radiation. The yields of ssb calculated from these dose dependencies are shown in Table 3 together with the photon energies of the radiation. These yields of homogeneous OH radicals were calculated by normalizing the yield of ssb for a given radiation relative to the yield for ^{60}Co γ-ray and taking $G(OH) = 0.29$ μmol J^{-1} for ^{60}Co γ radiation at 10^{-6} s.[41]

The dependence of the yield of homogeneously distributed OH radicals on photon energy is illustrated in Figure 2. The

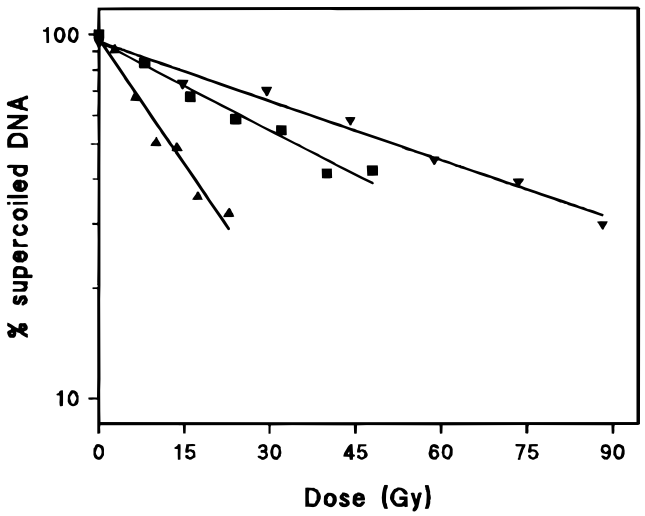

Figure 1. Dose dependence for the loss of supercoiled plasmid determined for varying incident energy photons. Irradiations were undertaken in an aqueous solution containing pUC18 and 0.66 mmol dm^{-3} Tris: (▼) aluminum USX; (■) diagnostic 50 kV (constant potential) X-ray; (▲) ^{60}Co γ-ray.

TABLE 3: Variation in the Yield of Single Strand Breaks Produced in PUC18 DNA with Incident Photon Energy

	energy	single strand break yield/Gy/Da	yield of OH radicals[a] (μmol J^{-1})
γ ^{60}Co	1.25 MeV av	18.80×10^{-9}	0.290
Ti X-ray K-shell emission	4.55 keV	5.81×10^{-9}	0.090
Al X-ray K-shell emission	1.49 keV	4.66×10^{-9}	0.072
Cu X-ray L-shell emission	0.96 keV	5.3×10^{-9}	0.082
C X-ray K-shell emission	0.28 keV	16.66×10^{-9}	0.257
Siemens Stabilipan 1 X-ray set	250 kV (const pot.) 90 keV av	15.31×10^{-9}	0.236
TODD Research machine Machlett X-ray set	50 kV (const pot.) 23 keV av	13.03×10^{-9}	0.201

[a] $G(OH)_{radiation}/G(OH)_{Co-60\ \gamma-rays} = (ssb/Gy/Da)_{radiation}/(ssb/Gy/Da)_{Co-60\ \gamma-rays}$.

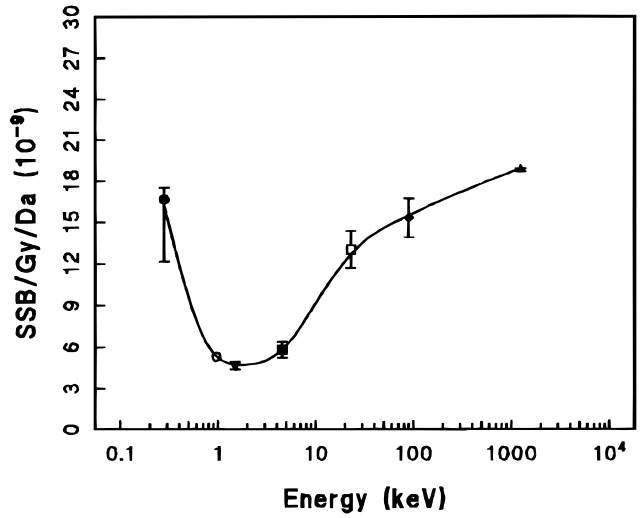

Figure 2. Experimental dependence of the yield of single strand breaks determined in pUC18 DNA with incident photon energy: (●) carbon USX; (○) Cu USX; (▼) aluminum USX; (■) titanium USX; (□) TODD Research X-ray set; (◆) Siemens X-ray set; (▲) ^{60}Co γ-ray.

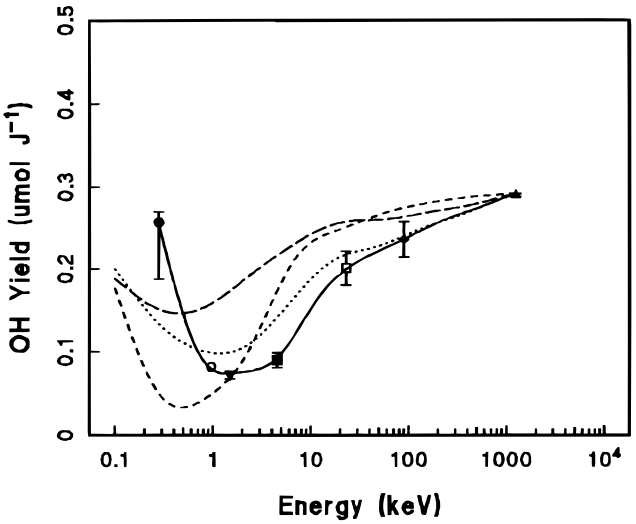

Figure 3. Comparison between the dependence on photon energy of the experimentally determined yields of OH radicals (see Table 3) and the simulated yields of OH radicals determined by Magee and Chatterjee[8] (- - -), Hill and Smith[7] (•••), and Yamaguchi[9] (— — —): (●) carbon USX; (○) Cu USX; (▼) aluminum USX; (■) titanium USX; (□) TODD Research X-ray set; (◆) Siemens X-ray set; (▲) ^{60}Co γ-ray.

yield of ssb/Gy/Da and therefore OH radicals increases with increasing photon energy for values of $E \geq 1$ keV. Below 1 keV the yield of ssb/Gy/Da and therefore OH radicals increases with decreasing photon energy. The attenuation of X-rays through the sample becomes increasingly important at lower energies (see Tables 1 and 2). An accurate determination of the sample thickness was obtained by confocal microscopy prior to irradiation. However, consideration must also be given to maintaining a constant sample thickness throughout the course of the experiment. Any evaporation during the course of the irradiation leads to variation in attenuation of the X-rays and consequently to a discrepancy between actual and assumed doses to the sample. The use of a cooled sample and dish, water droplets placed on top of the CR-39 disk, and a lid placed on top of the dishes minimizes such effects. These conditions are essential with the Cu_L and C_K USX as long irradiation times are required due to their low dose rates of 0.25 and 0.5 Gy $min^{-1,}$ respectively. Because of the low number of ssb/Gy/Da with Cu_L USX, long irradiation times are also required to give measurable breakage yields. Since the mass attenuation coefficients for Cu_L and C_K USX are similar in water (See Table 1), the difference in ssb yields between these two energies is directly indicative of a difference in OH radical yield and not dependent on assumptions in calculating mean doses through the samples.

Figure 3 shows comparisons between these experimentally determined yields of OH radicals with photon energy and those obtained from various theoretical simulations. In all cases there is some general agreement between the shapes of the curves for the simulated and experimentally determined dependencies, but there are some significant quantitative differences in the yields and in the positions of the minimum.

Discussion

The main finding is that the experimentally determined yield of ssb is dependent upon the photon energy of the radiations used. As the photon energy is reduced, there is a decrease in the number of ssb/Gy/Da to a minimum value at 1−2 keV, below which further decreases in photon energy result in an increased number of ssb/Gy/Da. The scavenging capacity of 0.66 mmol dm^{-3} Tris corresponds to a time of 1 μs, sufficiently long for OH radicals to become homogeneously distributed. The plasmid is also at a low concentration and thus both Tris and DNA are at concentrations insufficient to influence intratrack, radical−radical interactions but sufficiently high to interact with the majority of homogeneous OH radicals in competition with their loss by intertrack radical−radical interactions. Since the plasmid is at a low concentration, it should be noted that an absolute measure of the number of radicals present is not obtained but the number of radicals is sampled for comparison between different radiation energies. From simulations with electrons of energy >1 keV, the initial yield of ionization and excitations is independent of the electron energy.[1,3] Therefore, observed differences in ssb yields on photon energy do not arise from differences in initial OH radical yields but reflect differences in the number of OH radicals that become homogeneously distributed. Thus, the number of ssb induced in plasmid DNA is proportional to the number of OH radicals escaping intratrack events and becoming homogeneously distributed. Differences in the homogeneously distributed yield of OH radicals are dependent upon the photon energy of the radiation and are therefore a reflection of the relative spatial distributions of the species that are formed within the radiation track.

When these results are compared with those obtained experimentally from Fricke dosimetric methods ($\geq$2 keV)[42] and from theoretical calculations,[7−9] there is partial agreement. However, with Fricke dosimetry, the yield of Fe^{3+} is determined from the interaction of Fe^{2+} with H atoms and OH radicals and the molecular product, H_2O_2. Therefore, the yield of OH radicals is not directly determined using the Fricke system. The reaction with H_2O_2 potentially compensates for any reduction in the yield of OH radicals as a result of intratrack recombination events. In Figure 3 the experimental dependence of OH radical yields on photon energy (Table 3) has been compared with various theoretical simulations for electrons or photons. The calculation of Magee and Chatterjee[8] for monoenergetic electrons and Yamaguchi[9] for monoenergetic photons both used a prescribed diffusion model. The tracks were broken up into a finite number of track entities in which the diffusion-controlled reaction kinetics were described using a set of simultaneous differential equations and an assumed distribution of radicals. These simulations were essentially fitted to the limited high-energy

electron and photon experimental data. The Monte Carlo electron simulations of Hill and Smith[7] followed the evolution of events, from the initial interactions to production of chemically reactive species to their subsequent diffusion-controlled reactions. The Monte Carlo method allows the stochastic nature of the radiation tracks to be followed.

In the case of the Magee and Chatterjee model,[8] the general shape of the response is similar to that obtained experimentally but the actual response is shifted toward lower energies, with the minimum OH radical yield occurring at 0.5 keV compared with the experimental value at ~1.5 keV. In comparison, with the Hill and Smith model (at 10^{-6} s),[7] a minimum occurs at approximately 1 keV with the depth similar to that determined experimentally. In addition, the subsequent rise in OH radical yields at the lower energies is less steep than that found experimentally. In the Yamaguchi model[9] a minimum occurs at a value similar to the Magee and Chatterjee model at around 0.5 keV. Over the entire energy range, the simulated OH radical yield[9] shows less of a dependence upon energy than the dependence determined either by experimental methods or by the other two models[7,8] examined. Some differences in yields between photons and electrons of a given energy are to be expected when the photon interaction results in two electrons (photon and Auger) of lower energies.

In summary, the decrease in the number of OH radicals escaping intratrack radical−radical interactions in the energy range of the photons from 1.25 MeV to 1.5 keV is a good indication of an increase in ionization density of the track with decreasing energy. In biological systems such increases in ionization density with decreasing energy of incident radiation would be expected to lead to a corresponding increase in complexity of DNA damage, resulting from local clustering of ionizations on the scale of DNA and its immediate surroundings.[21] Indeed, this track ionization density analysis is supported by experimental findings of an increase in the number of DNA double strand breaks,[18,43] which represent the simplest form of complex damage within cells, with decreasing photon energy of the radiation.

Acknowledgment. This study was partially supported by the Commission of the European Community, Contract no. F14-CT95-0011c.

References and Notes

(1) Pimblott, S. M.; LaVerne, J. A. *J. Phys. Chem. A* **1997**, *101*, 5828.
(2) Pimblott, S. M.; Green, N. J. B. In *Recent advances in the kinetics of radiolytic processes;* Compton, R. G., Hancock, G., Eds.; Elsevier: Amsterdam, 1995; Vol 3, pp 117−174.
(3) Pimblott, S. M.; LaVerne, J. A. *Radiat. Res.* **1998**, *150*, 159.
(4) LaVerne, J. A.; Pimblott, S. M. *Radiat. Res.* **1993**, *135*, 16.
(5) Pimblott, S. M. *J. Phys. Chem.* **1992**, *96*, 4485.
(6) Moiseenko, V. V.; Hamm, R. N.; Walker, A. J.; Prestwich, W. V. *Int. J. Radiat. Biol.* **1998**, *74*, 533.
(7) Hill, M. A.; Smith, F. A. *Radiat. Phys. Chem.* **1994**, *43*, 265.
(8) Magee, J. L.; Chatterjee, A. *J. Phys. Chem.* **1978**, *82*, 2219.
(9) Yamaguchi, H. *Radiat. Phys. Chem.* **1989**, *34*, 801.
(10) Watanabe, R.; Usami, N.; Kobayashi, K. *Int. J. Radiat. Biol.* **1995**, *68*, 113.
(11) Heida, K.; Suzuki, K.; Hirona, T.; Suzuki, M.; Furusawa, Y. *J. Radiat. Res.* **1994**, *35*, 104.
(12) Jonah, C. D.; Matheson, M. S.; Millar, J. R.; Hart, E. J. *J. Phys. Chem.* **1976**, *80*, 1267.
(13) Jonah, C. D.; Hart, E. J.; Matheson, M. S. *J. Phys. Chem.* **1973**, *77*, 1838.
(14) Yamaguchi, H. In *Microdosimetry: An Interdisciplinary Approach;* Goodhead, D. T., O'Neill, P., Menzel, H. G., Eds.; The Royal Society of Chemistry: Cambridge, U.K., 1997; pp 97−100.
(15) Nikjoo, H.; Goodhead, D. T. *Phys. Med. Biol.* **1991**, *36*, 229.
(16) Goodhead, D. T.; Nikjoo, H. *Int. J. Radiat. Biol.* **1989**, *55*, 513.
(17) Kobayashi, K.; Heida, K.; Maezawa, H.; Ando, M.; Ito, T. *J. Radiat. Res.* **1987**, *28*, 243.
(18) Botchway, S. W.; Stevens, D. L.; Hill, M. A.; Jenner, T. J.; O'Neill, P. *Radiat. Res.* **1997**, *148*, 317.
(19) Goodhead, D. T.; Thacker, J. *Int. J. Radiat. Biol.* **1977**, *31*, 541.
(20) Goodhead, D. T.; Nikjoo, H. *Radiat. Prot. Dosim.* **1990**, *31*, 343.
(21) Nikjoo, H.; O'Neill, P.; Goodhead, D. T.; Terrissol, M. *Int. J. Radiat. Biol.* **1997**, *71*, 467.
(22) Hodgkins, P. S.; O'Neill, P.; Stevens, D. L.; Fairman, M. P. *Radiat. Res.* **1996**, *146*, 660.
(23) Hodgkins, P. S.; Fairman, M. P.; O'Neill, P. *Radiat Res.* **1996**, *145*, 24.
(24) Milligan, J. R.; Aguilera, J. A.; Wu, C. C. L.; Ng, J. Y-Y.; Ward, J. F. *Radiat. Res.* **1996**, *145*, 442.
(25) Jonah, C. D.; Miller, J. R. *J. Phys. Chem.* **1977**, *81*, 1974.
(26) Sambrook, J.; Fritsch, E. F.; Maniatis, T. *Molecular Cloning, A Laboratory Manual*, 3rd ed.; Cold Spring Harbor Laboratory Press: New York, 1989.
(27) Townsend, K. M. S.; Stretch, A.; Stevens, D. L.; Goodhead, D. T. *Int. J. Radiat. Biol.* **1990**, *58*, 499.
(28) Hill, M. A.; Vecchia, M. D.; Townsend, K. M. S.; Goodhead, D. T. *Phys. Med. Biol.* **1998**, *43*, 351.
(29) Jones, G. D. D.; Boswell, T. V.; Ward, J. F. *Radiat. Res.* **1994**, *138*, 251.
(30) Tomita, H.; Kai, M.; Kusama, T.; Ito, A. J. *Radiat. Res.* **1995**, *36*, 46.
(31) Ito, T.; Baker, S. C.; Stickley, C. D.; Peak, J. G.; Peak, M. J. *Int. J. Radiat. Biol.* **1993**, *63*, 289.
(32) Milligan, J. R.; Aguilera, J. A.; Ward, J. F. *Radiat. Res.* **1993**, *133*, 151.
(33) Hoshi, M.; Goodhead, D. T.; Brenner, D. J.; Bance, D. A.; Chmielewski, J. J.; Paciotti, M. A.; Bradbury, J. N. *Phys. Med. Biol.* **1985**, *30*, 1029.
(34) Goodhead, D. T.; Thacker, J.; Cox, R. *Int. J. Radiat. Biol.* **1979**, *36*, 101.
(35) Goodhead, D. T.; Thacker, J.; Cox, R. *Phys. Med. Biol.* **1981**, *26*, 1115.
(36) Neary, G. J. In *The uses of Cyclotrons in Chemistry, Metallurgy and Biology*; Amphlett, C. B., Ed.; Butterworth: London, 1970; pp 194−203.
(37) Storm, E.; Israel, H. I. *Nucl. Data Tables* **1970**, *A7*, 565.
(38) ICRU. *Linear Energy Transfer*; ICRU Report 16; IRCU: Washington, DC, 1970.
(39) Henke, B. L.; Gullikson, E. M.; Davis, J. C. *At. Data Nucl. Data Tables* **1993**, *54*, 181.
(40) Buxton, G. V.; Greenstock, C. L.; Helman, W. P.; Ross, A. B. *J. Phys. Chem. Ref. Data* **1988**, *17*, 513.
(41) *Radiation Chemistry Principles and Applications;* Farhataziz, Rodgers, M. A. J., Eds.; VCH Publications Inc.: Deerfield Beach, FL, 1987.
(42) Freyer, J. P.; Schiliiaci, M. E.; Raju, M. R. *Int. J. Radiat. Biol.* **1989**, *56*, 885.
(43) Cunniffe, S.; O'Neill, P. *Radiat. Res.* **1999**, *152*, 421.